Formation Features of Hybrid Magnetic Materials Based on Polyphenoxazine and Magnetite Nanoparticles

S.Zh. Ozkan[1,*], G.P. Karpacheva[1], E.L. Dzidziguri[2], P.A. Chernavskii[3], G.N. Bondarenko[1] and G.V. Pankina[3]

[1]*A.V. Topchiev Institute of Petrochemical Synthesis, Russian Academy of Sciences, 29 Leninsky prospect, Moscow 119991, Russia*

[2]*National University of Science and Technology MISIS, 4 Leninsky prospect, Moscow 119049, Russia*

[3]*Department of Chemistry, Lomonosov Moscow State University, 1-3 Leninskie Gory, Moscow 119991, Russia*

Abstract: Hybrid metal-polymer nanocomposite materials based on polyphenoxazine (PPhOA) and Fe_3O_4 nanoparticles were obtained for the first time via two methods: *in situ* oxidative polymerization of phenoxazine (PhOA) in an aqueous solution of isopropyl alcohol with nanoparticles of Fe_3O_4 being present; chemical transformations of PPhOA subjected to IR heating at 400–450 °C in the presence of $FeCl_3 \cdot 6H_2O$ in an inert atmosphere. Obtained hybrid Fe_3O_4/PPhOA nanomaterials were characterized by means of Fourier transform infrared (FTIR) spectroscopy, X-ray diffraction (XRD), transmission electron microscopy (TEM), atomic absorption spectrometry (AAS), elemental analysis, differential scanning calorimetry (DSC), thermogravimetric analysis (TGA), as well as by vibrating sample magnetometry. The chemical structure, phase composition, magnetic and thermal properties of obtained nanocomposites were investigated in relation to the synthesis conditions.

Keywords: Polyphenoxazine, Conjugated polymers, Oxidative polymerization *in situ*, IR heating, Metal-polymer nanocomposite, Magnetic material, Fe_3O_4 nanoparticles.

INTRODUCTION

Hybrid polymer nanomaterials can be singled out from other prospective materials due to their unique physico-chemical properties [1-4]. Among these, the ones with the organic component presented by a polymer with conjugated system and the inorganic component presented by a magnetic nanoparticle are of particular interest. The interaction of nanoparticles and the polymer matrix ensures the multifunctionality of such nanomaterials. Hybrid nanomaterials based on conjugated polymers can reveal splendid electrical, optical, magnetic and electrochemical properties. They are promising for use in healthcare, systems of information storage, electromagnetic screens, contrasting materials for magnetic resonance imaging, electromechanical microsystems, sensors and biosensors, supercapacitors, displays, and other electrochemical devices.

The most effective method of synthesis for the metal-polymer nanocomposites is *in situ* oxidative polymerization of monomers (aniline, pyrrole) in reaction media containing magnetic nanoparticles (Fe_3O_4, γ-Fe_2O_3, α-Fe_2O_3, Co_3O_4) in the presence of oxidizers (H_2O_2, $(NH_4)_2S_2O_8$, $FeCl_3$) [5-13]. Such hybrid nanomaterials usually reveal superparamagnetic properties due to small dimensions and high dispersity of magnetic nanoparticles. Their saturation magnetization M_S is within the range 0.06–80.4 emu/g [6, 8, 14-16] depending on the composition of the material; it grows along with the content of nanoparticles.

Earlier we have prepared nanostructured magnetic materials based on polydiphenylamine-2-carboxylic acid and Fe_3O_4 nanoparticles by polymerization of diphenylamine-2-carboxylic acid in an alkaline medium of Fe_3O_4 nanoparticles synthesis, or alternatively under the interfase conditions [17-19]. Monomer is anchored to the Fe_3O_4 surface by means of binding the carboxylate ion with Fe resulting in the Fe-OOC bond. The saturation magnetization M_S is 27.5–33.5 emu/g. The hybrid nanomaterial obtained under the conditions of *in situ* interfase polymerization is a superparamagnetic with the content of superparamagnetic particles being close to 100% (hysteresis loop squareness coefficient k_S = 0.007). Other superparamagnetic nanomaterials ($k_S < 0.1$) based on polydiphenylamine [20-22] or polyphenoxazine [23-25] and Co nanoparticles [20, 21, 23, 24], Co-Fe nanoparticles [25] or those of Fe_3O_4 [22] have been prepared under the conditions of IR heating. Obtained values of k_S are typical for uniaxial, single-

---

[*] Address correspondence to this author at the A.V. Topchiev Institute of Petrochemical Synthesis, Russian Academy of Sciences, 29 Leninsky prospect, Moscow 119991, Russia; E-mail: ozkan@ips.ac.ru

E-ISSN: 1929-5995/16

domain particles. For Co and Fe_3O_4 the critical dimension of the single-domain state is 20 and 128 nm respectively [26, 27].

In this paper hybrid magnetic nanocomposites based on polyphenoxazine (PPhOA) and Fe_3O_4 nanoparticles were prepared for the first time. The comparison was made regarding the structure and properties of nanocomposites obtained in two ways: via *in situ* oxidative polymerization of phenoxazine (PhOA) in an aqueous solution of isopropyl alcohol with nanoparticles of Fe_3O_4 being present; through chemical transformations of PPhOA subjected to IR heating in the presence of $FeCl_3 \cdot 6H_2O$. Magnetic and thermal properties of obtained nanomaterials were investigated.

EXPERIMENTAL

Phenoxazine (PhOA) (Acros Organics, 97%), isopropyl alcohol (high purity grade), toluene (analytical grade), dimethylformamide (DMF) (Acros Organics, 99%), $FeCl_3 \cdot 6H_2O$ (reagent grade), and $FeSO_4 \cdot 7H_2O$ (reagent grade) were used without any additional purification. Ammonium peroxydisulfate $(NH_4)_2S_2O_8$ (analytical grade) was purified by recrystallization. Aqueous solutions of the reactants were prepared with the use of distilled water.

Polyphenoxazine (PPhOA) was prepared via *in situ* oxidative polymerization of PhOA in an aqueous solution of isopropyl alcohol ($M_w = 2.4 \times 10^4$); also in an interfase process using a procedure developed by the authors and described in [28] ($M_w = 3.7 \times 10^4$). PPhOA is a blue powder, completely soluble in *N*-methylpyrrolidone, DMF, DMSO, dioxane, acetone, THF, chloroform.

Molecular weight of PPhOA was measured by gel permeation chromatography (GPC) on a Milton Roy instrument equipped with a Milton Roy RI-detector and a PLgel 5μm MIXED-C column using *N*-methylpyrrolidone as an eluent at 60 °C. The eluent flow rate was 1 ml/min. The volume of injected sample was 150 ml. Polystyrene was used for the calibration. The accuracy of M_W determination was ~ 5%.

Synthesis of Fe_3O_4/PPhOA nanocomposite via *in situ* oxidative polymerization was conducted in the following manner. First Fe_3O_4 nanoparticles were obtained by hydrolysis of iron (II) and (III) salts mixed at the ratio 1:2 in the ammonium hydroxide solution at 60 °C [18, 19, 29]. For this purpose, 0.11–0.86 g of $FeSO_4 \cdot 7H_2O$ and 0.29–2.35 g of $FeCl_3 \cdot 6H_2O$ were dissolved in 20 ml of distilled water, heated to 60 °C, and then 5 ml of NH_4OH were introduced to the solution. The obtained suspension was heated in water bath to 80 °C with mixing for 0.5 h, then cooled to the room temperature while being mixed intensively for 1 h. In order to anchor the monomer on the surface of Fe_3O_4 the nanoparticles were filtered, rinsed with distilled water up to the neutral reaction of the filtrate, and (without any preliminary drying) introduced into the PhOA solution of 0.1 mol/l (0.55 g) in isopropyl alcohol (15 ml) at 60 °C and intense mixing for 1 h. The resulting suspension (Fe_3O_4/PhOA in isopropyl alcohol) was likewise cooled to the room temperature while being mixed intensively for 1 h, then down to 0 °C with continuous intense mixing. In order to conduct *in situ* oxidative polymerization of PhOA in neutral media on the surface of Fe_3O_4 nanoparticles, an aqueous solution of ammonium peroxydisulfate of 0.125 mol/l (0.86 g) was introduced by drops. The volume ratio of aqueous and organic phases was 1:1 (at total volume 30 ml). The polymerization reaction was conducted for 3 h at 0 °C with continuous intense mixing. Upon ending, the product was filtered, rinsed several times with distilled water in order to make it reactant-free, and dried under vacuum over KOH until the stabilization of weight. The yield of Fe_3O_4/PPhOA nanocomposite was 0.54 and 1.18 g for [Fe] contents of 15.1 and 59.6% respectively (according to atomic absorption spectrometry (AAS) data, Tables **1, 2**). When Fe_3O_4/PPhOA nanocomposite was dispersed in ethyl alcohol, its sedimentation began from the first minutes. The resulting black precipitate revealed magnetic properties when a magnet was put close to it.

In order to synthesize Fe_3O_4/PPhOA nanocomposite by IR heating, the joint solution was prepared which contained PPhOA obtained in an interfase process and iron (III) chloride $FeCl_3 \cdot 6H_2O$ dissolved in DMF. Concentration of PPhOA in the DMF solution was 2 wt%, the content of [Fe] was 5–30 wt% of the polymer weight (not taking the acidic residue into consideration). The precursor (PPhOA and iron (III) chloride) was prepared by evaporation of the solvent (DMF) at 60–85 °C. It was heated by IR radiation in Ar atmosphere at 400–450 °C for 2–10 min using an automatic device of IR heating described in [30]. Heating rate was 50 °C/min. The yield of Fe_3O_4/PPhOA nanocomposite was (depending on the synthesis conditions) 76–89% at [Fe] content 10–26% (according to AAS data, Tables **1, 2**). The obtained metal-polymer Fe_3O_4/PPhOA nanocomposite had the appearance of a black powder which did not dissolve in organic solvents such as N-methylpyrrolidone, DMF, DMSO.

Table 1: Atomic-Absorption Spectrometry Data of Fe_3O_4/PPhOA Nanocomposites and Elemental Analysis Data of PPhOA

Synthesis method	*T*, °C	Fe, %	C, %	N, %	H, %	O, %
In situ oxidative polymerization	0	-	78.7*	7.7	4.9	8.7
		15.1	61.7	5.6	3.4	14.2
		59.6	25.2	2.1	1.6	11.5
IR heating	400	9.9**	61.7	7.1	2.7	18.6
		17.2***	54.6	6.0	1.9	20.3

*Initial PPOA, **[Fe] = 10 wt% (at the loading), ***[Fe] = 20 wt%.

Table 2: Magnetic Characteristics of Fe_3O_4/PPOA Nanocomposites

Synthesis method	*T*, °C	[Fe], %	H_C, Oe	M_S, emu/g	M_R, emu/g	M_R/M_S
In situ oxidative polymerization	0	15.1	0	11.43	0	0
		59.6	5	49.21	0.75	0.015
IR heating	400	17.2*	269	19.35	5.3	0.274
		25.9**	223	25.52	7.6	0.298

*[Fe] = 20 wt% (at the loading), **[Fe] = 30 wt%.
H_C – coercive force, M_S – saturation magnetization, M_R – residual magnetization, k_S – the hysteresis loop squareness coefficient.

The content of metal in Fe_3O_4/PPhOA nanocomposite was determined quantitatively by AAS using Carl Zeiss Jena AAS 30 spectrophotometer (Tables **1, 2**). Fe content was measured with accuracy ±1%.

Fourier transform infrared (FTIR) spectra of PPhOA and Fe_3O_4/PPhOA nanocomposite were recorded in the range 400–4000 cm^{-1} using IFS 66v Bruker FTIR spectrometer and processed with the Soft-Spectra software. The samples were dispersed in KBr and compressed into pellets.

X-ray diffraction (XRD) studies were performed at room temperature using Difray X-ray diffractometer with Bragg-Brentano focus on CrK_α-radiation. The diffraction patterns were used to calculate the size distribution of the coherent scattering regions of the crystallites [31] in Fe_3O_4 nanoparticles.

Transmission electron microscopy (TEM) microphotographs were taken on a Leo912 AB Omega transmission electron microscope. Size of nanoparticles was determined using the EsiVision software.

A vibration magnetometer was used to study the magnetic characteristics of the samples. The cell of the vibration magnetometer was designed as a flow quartz microreactor, which allowed studying the chemical transformations in the *in situ* mode [27]. Magnetization of a sample was recorded as function of the value of the magnetic field at room temperature.

Thermogravimetric analysis (TGA) of PPhOA and Fe_3O_4/PPhOA nanocomposite was performed on TGA/DSC1 unit by Mettler Toledo in a dynamic mode in the range 30–1000 °C under air and inert nitrogen conditions. The loading of the polymer was 100 mg, heating rate – 10 °C/min, nitrogen flow – 10 ml/min. Calcined aluminum oxide was used as a reference. Sample analysis was carried out in an Al_2O_3 crucible.

Differential scanning calorimetry (DSC) was carried out on DSC823e calorimeter by Mettler Toledo. Heating rate was 10 °C/min in Ar flow (70 ml/min). The results were processed with a service program STARe given with the device.

RESULTS AND DISCUSSION

Synthesis of hybrid metal-polymer nanocomposite materials based on PPhOA and Fe_3O_4 nanoparticles was performed by two methods: *in situ* oxidative polymerization of PhOA in an aqueous solution of isopropyl alcohol with nanoparticles of Fe_3O_4 being present; IR heating of PPhOA in the presence of iron (III) chloride $FeCl_3 \cdot 6H_2O$. PPhOA synthesized by the authors for the first time is a semi-ladder heterocyclic polymer which contains nitrogen and also oxygen atoms participating in the common system of polyconjugation [28]. Analyses made by FTIR, nuclear magnetic resonance, electron and X-ray photoelectron spectroscopy allowed to visualize the chemical structure of PPhOA as follows:

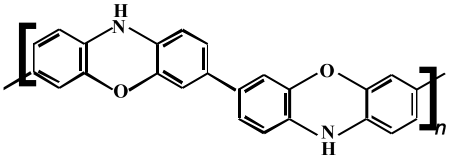

Formation of hybrid metal-polymer nanocomposite materials based on PPhOA and Fe_3O_4 nanoparticles in the course of *in situ* oxidative polymerization of PhOA in an aqueous solution of isopropyl alcohol in the presence of Fe_3O_4 nanoparticles includes: synthesis of Fe_3O_4 nanoparticles by hydrolysis of iron (II) and (III) salts mixed at the ratio 1:2 in a solution of ammonium hydroxide; anchoring of the monomer (PhOA) on the surface of these nanoparticles in the reaction media of the nanocomposite synthesis; *in situ* polymerization in neutral media in the presence of oxidizer (an aqueous solution of ammonium peroxydisulfate).

Synthesis of hybrid metal-polymer nanocomposite materials based on PPhOA and Fe_3O_4 nanoparticles by IR heating was achieved through chemical transformations of PPhOA subjected to IR radiation in the presence of iron (III) chloride $FeCl_3 \cdot 6H_2O$ in an inert atmosphere. For these purposes PPhOA obtained under the interfase conditions was used. The use of IR radiation allowed to increase the rates of chemical reactions notably, thus, to decrease the process duration.

Formation of Fe_3O_4/PPhOA nanocomposite materials was confirmed by TEM, FTIR, XRD, AAS.

Figures **1** and **2** depict the FTIR spectra of Fe_3O_4/PPhOA nanocomposites obtained via *in situ* oxidative polymerization and IR heating, respectively. Table **3** presents the attribution of the main characteristic bands in the spectra of PPhOA and nanocomposites. A comparison of IR spectra of polymer and nanocomposite obtained by *in situ* oxidative polymerization shows that the spectra of nanocomposite have all the main bands which

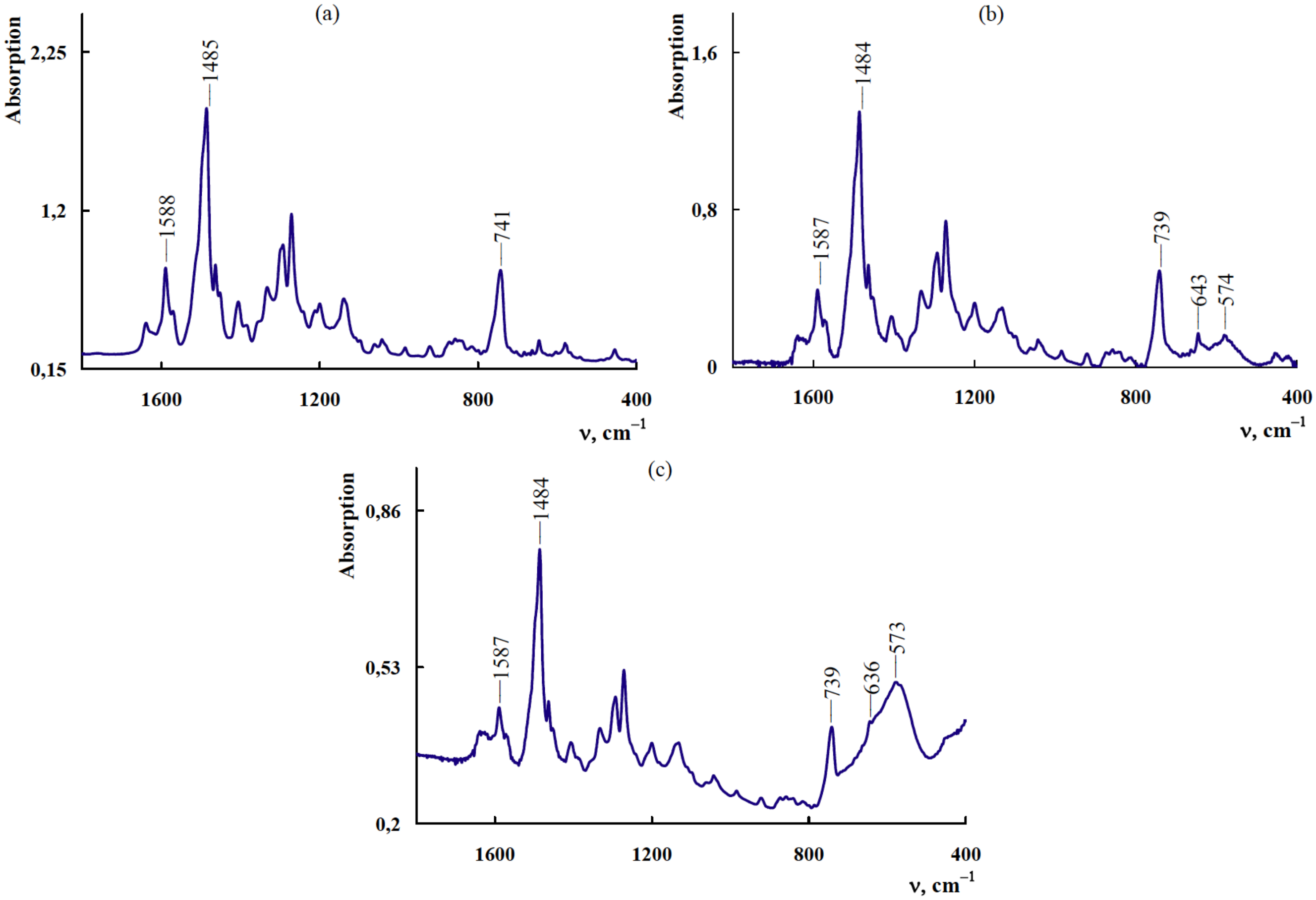

Figure 1: FTIR spectra of PPhOA (**a**) and Fe_3O_4/PPhOA nanocomposite prepared by *in situ* oxidative polymerization at [Fe] = 15.1 (**b**) and 59.6% (**c**).

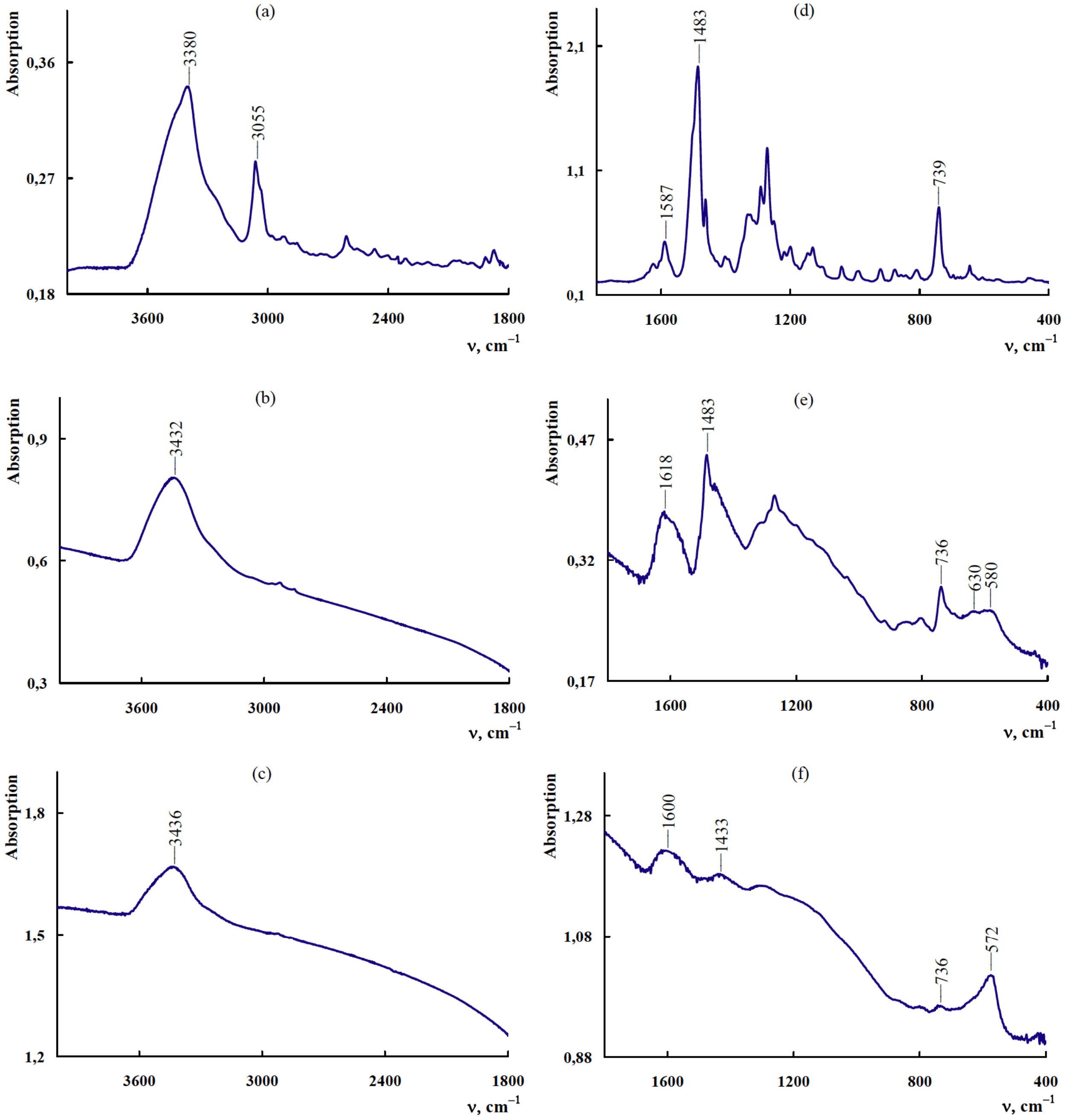

Figure 2: FTIR spectra of PPhOA (**a**, **d**) and Fe_3O_4/PPhOA nanocomposite prepared by IR heating at 400 °C for 2 min at Fe content (at the loading) 10 (**b**, **e**) and 20 wt% (**c**, **f**).

characterize the chemical structure of the initial polymer (Figure **1**, Table **3**). As in the case of PPhOA, the growth of the polymer chain in the nanocomposite occurs by C–C- joining to phenyl rings in the *para*-position regarding to nitrogen. The PPhOA structure contains only benzoid amine groups [28]. A characteristic change for the IR spectra of Fe_3O_4/PPhOA nanocomposite compared to that of the initial polymer (synthesized in an aqueous solution of isopropyl alcohol) is the presence of the absorption band at 573 cm^{-1}, corresponding to the stretching vibrations of $\nu_{Fe–O}$ bonds (Figure **1**). Naturally, an increase in the content of Fe_3O_4 in the nanocomposite leads to a significant increase in the intensity of the band at 573 cm^{-1}, characterizing $\nu_{Fe–O}$ bonds.

XRD study of the structure of Fe_3O_4/PPhOA nanocomposite material obtained via *in situ* oxidative polymerization allowed to determine that the only phase in this material with presence of metal is Fe_3O_4, identified clearly by broad peaks of diffraction in the range of scattering angles 2θ = 45.8°, 54.0°, 66.7°,

Table 3: Attribution of the Main Characteristic Absorption Bands in FTIR Spectra of the Studied Materials

Attribution of absorption bands	Frequency v, cm^{-1}			
	PPhOA		Fe_3O_4/PPhOA	
	In situ oxidative polymerization			IR heating
	in a solution of isopropyl alcohol	in an interfase process	in a solution of isopropyl alcohol	
Stretching vibrations $\nu_{N–H}$	3380	3380	-	-
Stretching vibrations $\nu_{C–H}$ in an aromatic ring	3055	3055	3055	-
Stretching vibrations $\nu_{O–H}$ in H_2O	-	-	3418	3436
Stretching vibrations $\nu_{C–C}$ in an aromatic ring	1588, 1485	1587, 1483	1587, 1484	1600, 1433
Stretching vibrations $\nu_{C–N}$	1330, 1291, 1270	1326, 1290, 1270	1330, 1291, 1270	1291
Bending vibrations $\delta_{C–H}$ in an 1,2-substituted aromatic ring	741	739	739	736
Bending vibrations $\delta_{C–H}$ in an 1,2,4-substituted aromatic ring	869, 837	869, 836	869, 836	869
Stretching vibrations $\nu_{Fe–O}$	-	-	573	572

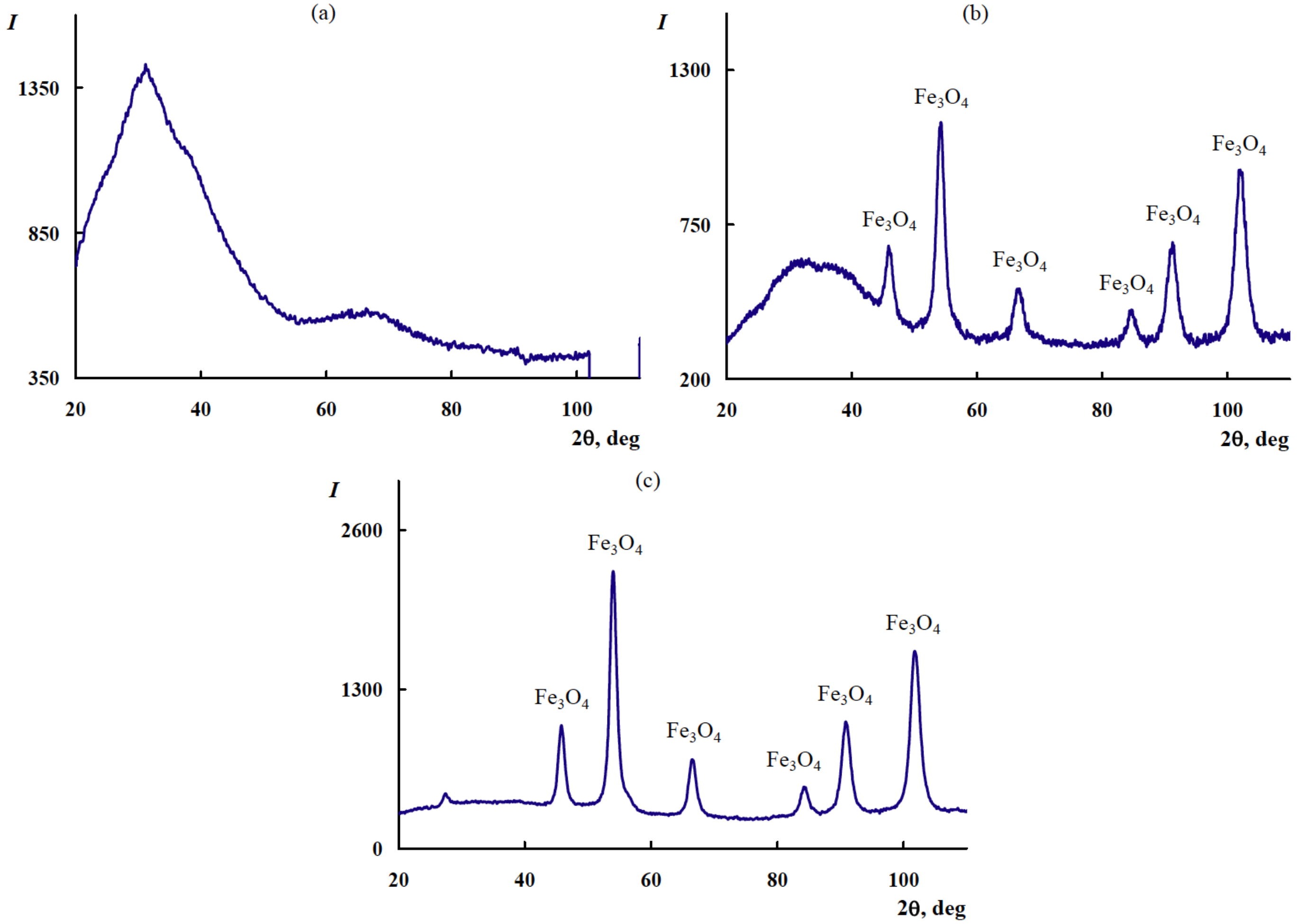

Figure 3: XRD diffractograms of PPhOA (**a**) and Fe_3O_4/PPhOA nanocomposite prepared by *in situ* oxidative polymerization at [Fe] = 15.1 (**b**) and 59.6% (**c**).

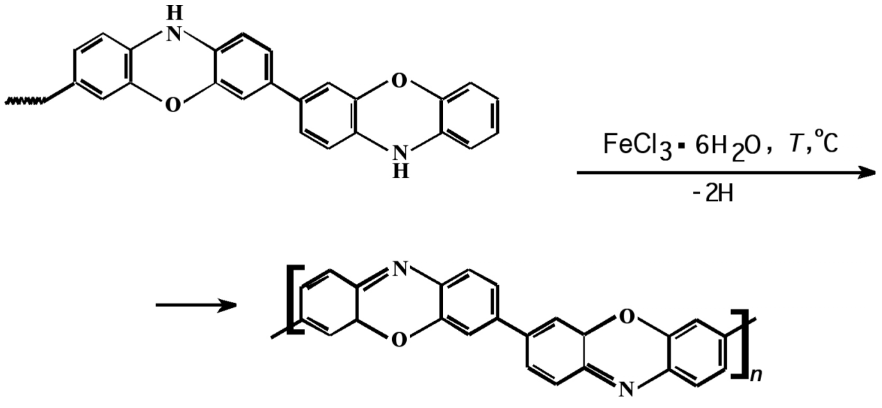

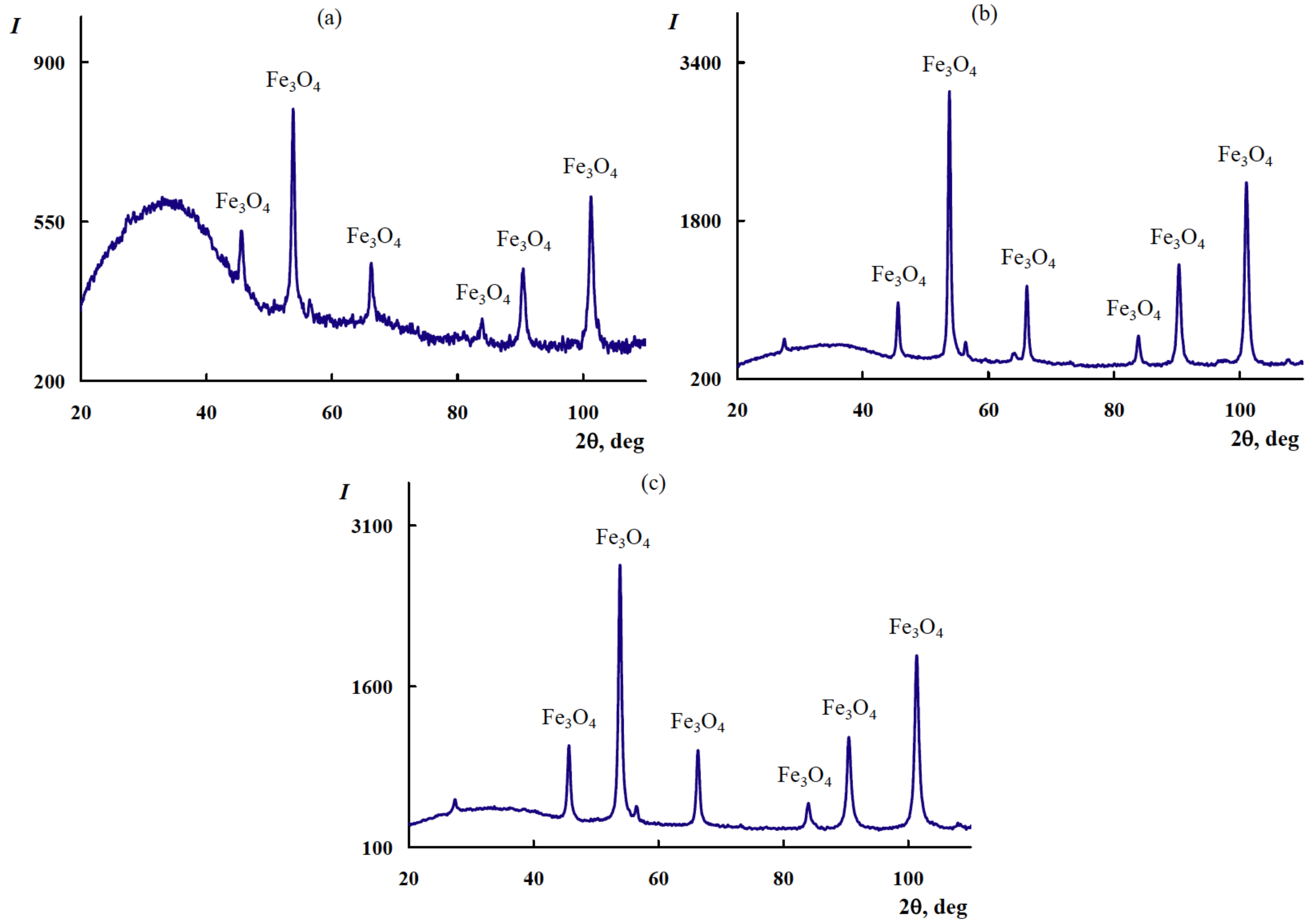

Figure 4: XRD diffractograms of Fe_3O_4/PPhOA nanocomposite prepared by IR heating at 400 °C for 2 min at Fe content (at the loading) 10 (**a**), 20 (**b**) and 30 wt% (**c**).

84.5°, 90.9° and 101.9° (CrK_α-radiation) (Figure **3**). These diffraction peaks correspond to the cubic structure of magnetite (JCPDS 19-0629) and refer respectively to indexes (220), (311), (400), (422), (511) and (440).

It was shown by FTIR spectroscopy that in the course of PPhOA heating by IR radiation at 400–450 °C in an inert atmosphere in the presence of $FeCl_3{\cdot}6H_2O$ the following reactions occur simultaneously: dehydrogenation of phenoxazine structures resulting in formation of C=N bonds, and metal reduction by released hydrogen resulting in formation of Fe_3O_4 nanoparticles.

According to FTIR data the proceeding of the former reaction (dehydrogenation of phenoxazine structures resulting in formation of C=N bonds) can be validated by the shift and broadening of the absorption bands at 1587 and 1483 cm^{-1} which relate to the stretching vibrations of ν_{C-C} bonds in aromatic rings (Figure **2**, Table **3**). Absorption bands at 3380 and 3055 cm^{-1}, corresponding to the stretching vibrations of ν_{N-H} and ν_{C-H} bonds in phenoxazine structures, are practically absent. New bands appear at 3436 and 572 cm^{-1}, related to the presence of water and to the stretching vibrations of ν_{Fe-O} bonds, respectively.

Elemental analysis data confirm decrease in hydrogen content in PPhOA in the presence of $FeCl_3 \cdot 6H_2O$ with temperature of IR heating growth (Table **1**). XRD data confirm that this hydrogen is active in Fe(III) reduction resulting in formation of magnetite in the form of nanoparticles. Diffractograms of Fe_3O_4/PPhOA nanocomposite obtained by IR heating show well-defined narrow diffraction peaks of Fe_3O_4 in the range of scattering angles 2θ = 45.66°, 53.8°, 66.16°, 83.95°, 90.36°, 101.1° (Figure **4**).

From XRD data the size distribution of Fe_3O_4 crystallites was obtained regarding to the coherent scattering regions. Figure **5** depicts such distribution depending on the chosen method of nanocomposite synthesis. For the first method (*in situ* oxidative polymerization), about 97% of Fe_3O_4 crystallites in Fe_3O_4/PPhOA nanocomposite are of size not exceeding 10 nm with the maximum of size distribution at 3 nm. According to TEM data the size of Fe_3O_4 nanoparticles is within the range $2 < d < 14$ nm (Figure **6a**). As is seen from Figure **5**, the second method (IR heating) produces Fe_3O_4/PPhOA nanocomposite with a broader size distribution curve; the maximum is at 11 nm, and the size of Fe_3O_4 nanoparticles by TEM is within the range $4 < d < 35$ nm.

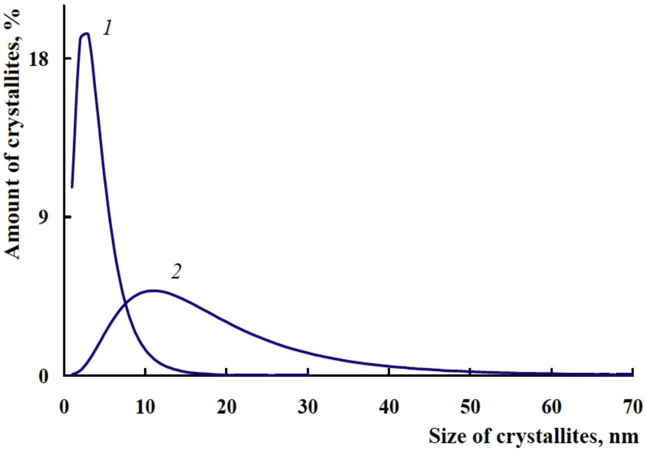

Figure 5: Fe_3O_4 crystallites size distribution in Fe_3O_4/PPhOA nanocomposites prepared by *in situ* oxidative polymerization (*1*) and by IR heating (*2*).

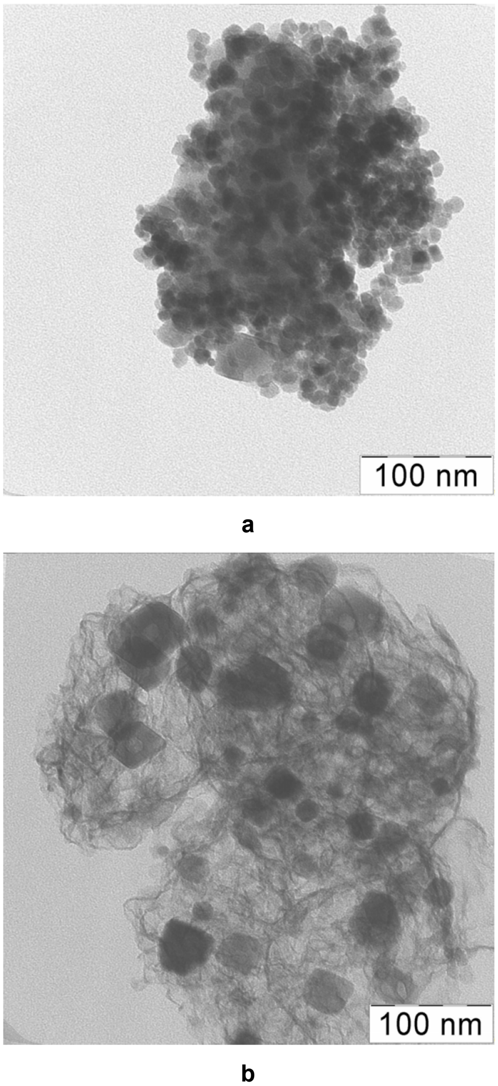

Figure 6: TEM images of Fe_3O_4/PPhOA nanocomposites prepared by *in situ* oxidative polymerization (**a**) and by IR heating at 600 °C (**b**).

The influence of synthesis conditions (method of synthesis, temperature, Fe concentration) on the phase composition of Fe_3O_4/PPhOA nanocomposites was investigated. It is found that the only metal-containing phase in the nanocomposite obtained by *in situ* oxidative polymerization is magnetite, regardless of Fe concentration (Figure **3**). As to the other method (IR heating at 400–450 °C for 2–10 min in an inert media), at Fe concentrations 5–30 wt% at the loading, only nanoparticles of magnetite are registered (Figure **4**). By increasing the iron concentration above 30 wt% at the loading or decreasing the temperature to 350 °C in the nanocomposite the degree of reduction is lower and Fe_2O_3 nanoparticles can be found as the result of less complete reduction along with those of magnetite. This is confirmed by the XRD reflection peaks of Fe_2O_3 in the range of diffraction angles 2θ = 36.4°, 50.3°, 62.7°, 77.3°, 85.2°, 104.4°. Temperatures above 450 °C cause further reduction of Fe_3O_4 to FeO and Fe, confirmed by diffraction peaks at 2θ = 55.1°, 64.5°, 98.04° (FeO) and 2θ = 68.87°, 106.28° (Fe). It was established that an increase in temperature leads to a change in morphology of Fe_3O_4 nanoparticles. Apart from spherical Fe_3O_4 nanoparticles, more coarse square Fe_3O_4 nanoparticles of sizes from 45 × 34 nm to 57 × 46 nm are formed (Figure **6b**). It is the result of high propensity of nanoparticles for aggregation [32].

Magnetic properties of Fe_3O_4/PPhOA nanocomposites depend heavily on the synthesis method. The dependence of the magnetization on the applied magnetic field is given in Figure **7**. The values of the main magnetic characteristics of nanocomposites are collected in Table **2**. As is seen from Figure **7**, for the samples obtained by *in situ* oxidative polymerization the hysteresis loop squareness coefficient $k_S = M_R/M_S \sim 0$, which testifies to the almost exclusive presence of superparamagnetic nanoparticles. The saturation magnetization M_S grows along with the content of Fe_3O_4 nanoparticles, achieving 49.21 emu/g at [Fe] = 59.6%. The residual magnetization M_R is 0–0.75 emu/g. The coercive force H_C is within the range 0–5 Oe.

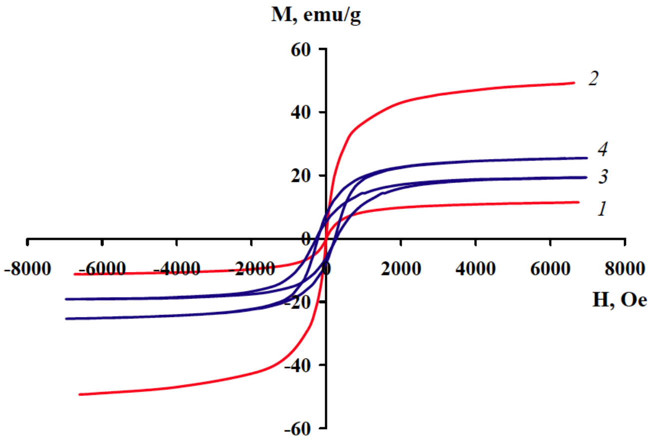

Figure 7: Dependence of magnetization on the applied magnetic field at room temperature for Fe_3O_4/PPhOA nanocomposites prepared by *in situ* oxidative polymerization (*1*, *2*) and by IR heating (*3*, *4*) at [Fe] = 15.1 (*1*), 59.6 (*2*), 17.2 (*3*) and 25.8% (*4*).

As is seen from Figure **7** and Table **2**, the use of IR heating for the synthesis of Fe_3O_4/PPhOA nanocomposites produces a large quantity of ferromagnetic particles – the coercive force H_C increases up to 269 Oe, while the hysteresis loop squareness coefficient $k_S = M_R/M_S$ increases as well up to 0.274–0.298. The saturation magnetization M_S depends on the concentration of Fe; it is within the range 19.35–25.92 emu/g at [Fe] = 17.2–25.9%. The residual magnetization M_R is 5.3–7.6 emu/g. Thus, the method of IR heating produces ferromagnetic nanocomposite materials.

Thermal stability of obtained Fe_3O_4/PPhOA nanocomposites was investigated by TGA and DSC. Figures **8** and **9** depict the temperature dependence of the weight of Fe_3O_4/PPhOA nanocomposites obtained via two methods (*in situ* oxidative polymerization; IR heating) in comparison with PPhOA when the samples are heated up to 1000 °C in the nitrogen flow and in air. Table **4** collects the values of the main thermal properties of the said materials.

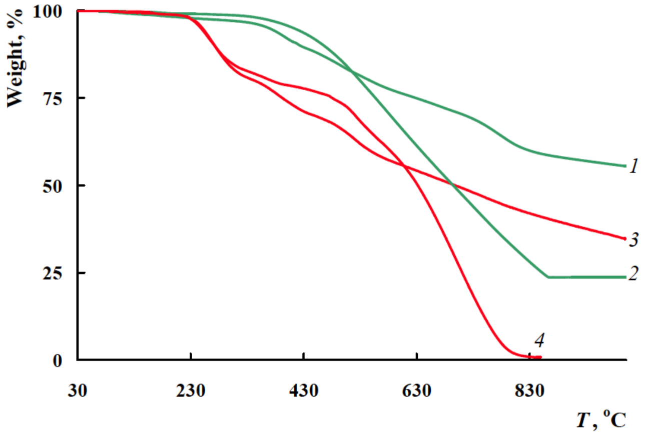

Figure 8: TGA thermograms of Fe_3O_4/PPhOA nanocomposite (*1*, *2*) and PPhOA (*3*, *4*) prepared by *in situ* oxidative polymerization in an aqueous solution of isopropyl alcohol at heating up to 1000 °C at the rate of 10 °C/min in the nitrogen flow (*1*, *3*) and in air (*2*, *4*).

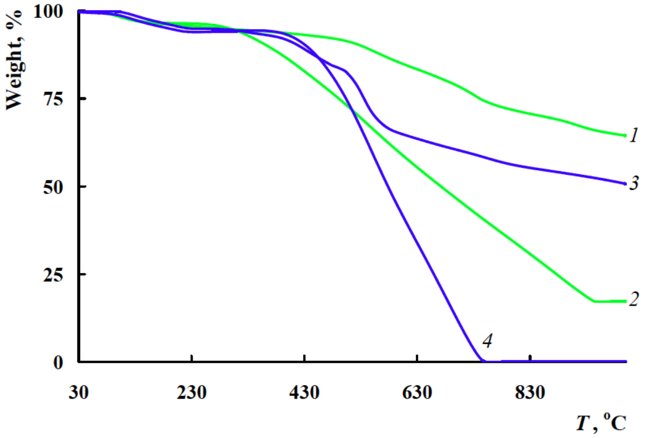

Figure 9: TGA thermograms of Fe_3O_4/PPhOA nanocomposite prepared by IR heating (*1*, *2*) and PPhOA (*3*, *4*) at heating up to 1000 °C at the rate of 10 °C/min in the nitrogen flow (*1*, *3*) and in air (*2*, *4*). PPhOA was obtained by *in situ* oxidative polymerization in an interfase process.

As is seen from Figure **8**, the weight loss is detected at 230 °C for PPhOA as opposed to Fe_3O_4/PPhOA

Table 4: Thermal Properties of the Studied Materials

Characteristics	PPhOA		Fe_3O_4/PPhOA	
	In situ oxidative polymerization			IR heating
	in a solution of isopropyl alcohol	in an interfase process	in a solution of isopropyl alcohol	
$^{*}T_{5\%}$, °C	248 / 250	189 / 224	411 / 367	297 / 283
$^{**}T_{50\%}$, °C	632 / 697	578 / >1000	694 / >1000	672 / >1000
***Residue, %	0 / 35	0 / 51	24 / 55	17 / 64

$^{*}T_{5\%}$, $^{**}T_{50\%}$ – temperatures of weight loss 5 and 50% (Air/Ar), ***residue at 1000 °C (Air/Ar).

nanocomposite obtained by *in situ* oxidative polymerization in an aqueous solution of isopropyl alcohol, the conditions of synthesis being the same for both compounds. This weight loss is due to the decomposition of low-molecular fraction present in the polymer, which is supported by DSC data. The DSC thermogram of PPhOA has an endothermic peak at 285 °C pointing at this decomposition (Figure **10**, curve **3**). The absence of such peak on the thermogram of polymer at the second heating writes off the possibility of melting at 285 °C. According to XRD data PPhOA is an amorphous polymer (Figure **3a**). The fact that the weight is not lost at this temperature in the case of Fe_3O_4/PPhOA nanomaterial obtained via *in situ* oxidative polymerization points at the anchoring of polymer on Fe_3O_4 nanoparticles.

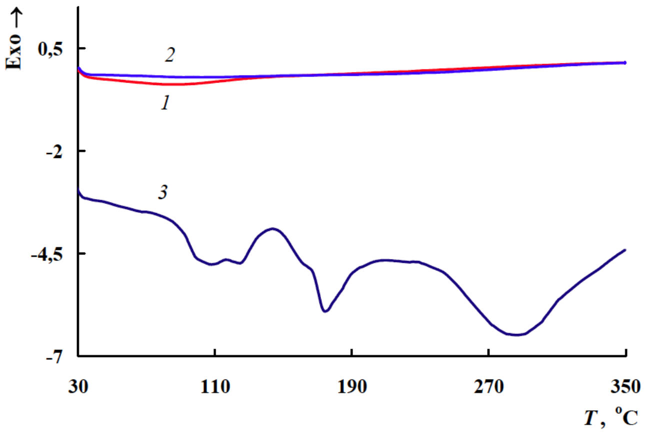

Figure 10: DSC thermograms of Fe_3O_4/PPhOA nanocomposite prepared by IR heating (*1*, *2*) and PPhOA (*3*) at heating in the nitrogen flow to 350 °C at the rate of 10 °C/min (*1, 3* – first heating, *2* – second heating).

Figure **9** refers to Fe_3O_4/PPhOA nanocomposite obtained by IR heating; may we remind that PPhOA in this case has been synthesized in an interfase process. As is seen from Figure **9**, after water removal the weight of the nanocomposite remains stable up to 310 °C. The absence of weight loss in the nanocomposite in this temperature range is connected to the processes which occur in the course of the nanocomposite synthesis, namely the condensation reaction where the polymer chain grows from the oligomers present in PPhOA [23]. By FTIR data, a conclusion on the growth of the polymer chain can be made from a decrease in intensity of the absorption band at 739 cm^{-1}, which refers to the bending vibrations of δ_{C-H} bonds in the 1,2-substituted benzene ring of the end groups – the lower the intensity, the lower the number of the said groups of polymer (Figure **2**).

As is seen from Figures **8**, **9** and Table **4**, Fe_3O_4/PPhOA nanocomposites prepared by two different methods (*in situ* oxidative polymerization; IR heating) lose half of their weight in air at 694 and 672 °C; at 1000 °C the initial weight dwindles to 24 and 17% respectively. In an inert media this process is much slower; at 1000 °C the respective percentage is 55 and 64%. For PPhOA samples obtained in an aqueous solution of isopropyl alcohol and in an interfase process at 1000 °C the residue is 35 and 51% respectively (Table **4**).

CONCLUSIONS

Hybrid nanocomposite materials based on polyphenoxazine and Fe_3O_4 nanoparticles were synthesized for the first time via two methods: *in situ* oxidative polymerization and IR heating. The structure, magnetic and thermal properties of obtained nanocomposites were investigated. It was established that the size of Fe_3O_4 nanoparticles and the magnetic properties of Fe_3O_4/PPhOA nanomaterials depend on the synthesis method. For the first method (*in situ* oxidative polymerization) the size of Fe_3O_4 nanoparticles is within the range $2 < d < 14$ nm. For the second method (IR heating) the size of Fe_3O_4 nanoparticles by TEM is within the range $4 < d < 35$ nm. For the samples obtained by *in situ* oxidative polymerization the hysteresis loop squareness coefficient $k_S = M_R/M_S \sim 0$, which reveals that almost 100% of Fe_3O_4 nanoparticles are superparamagnetic. The saturation magnetization M_S achieves 49.21 emu/g. The use of IR heating for the synthesis of Fe_3O_4/PPhOA nanocomposites produces a large quantity of ferromagnetic particles. The coercive force H_C increases up to 269 Oe, the hysteresis loop squareness coefficient $k_S = M_R/M_S = 0.298$, the saturation magnetization M_S is 25.92 emu/g. Obtained nanocomposites are of high thermal stability. Fe_3O_4/PPhOA nanocomposites prepared via two different methods (*in situ* oxidative polymerization; IR heating) lose half of their weight in air at 694 and 672 °C. In an inert media at 1000 °C the residue is 55 and 64% respectively.

ACKNOWLEDGMENTS

The authors express their sincere gratitude to G.A. Shandryuk (A.V. Topchiev Institute of Petrochemical Synthesis, RAS) for conducting the TGA, DSC analyses of Fe_3O_4/polyphenoxazine nanocomposites.

REFERENCES

[1] Sellinger A, Weiss PM, Nguyen A, *et al.* Continuous self-assembly of organic-inorganic nanocomposite coatings that mimic nacre. Nature 1998; 394: 256-60. https://doi.org/10.1038/28354

[2] Yamamoto K, Sakata Y, Nohara Y, Takahashi Y, Tatsumi T. Organic-inorganic hybrid zeolites containing organic frameworks. Science 2003; 300: 470-2. https://doi.org/10.1126/science.1081019

[3] Gerasin VA, Antipov EM, Karbushev VV, *et al.* New approaches to the development of hybrid nanocomposites: from structural materials to high-tech applications. Russ Chem Rev 2013; 82: 303-32. https://doi.org/10.1070/RC2013v082n04ABEH004322

[4] Pomogailo AD, Rozenberg AT, Uflyand IE. Metal nanoparticles in polymers Khimiya, Moscow, 2000; p. 672. [in Russian].

[5] Yang C, Du J, Peng Q, *et al.* Polyaniline/Fe_3O_4 nanoparticle composite: synthesis and reaction mechanism. J Phys Chem B 2009; 113: 5052-8. https://doi.org/10.1021/jp811125k

[6] Qiu G, Wang Q, Nie M. Polyaniline/Fe_3O_4 magnetic nanocomposite prepared by ultrasonic irradiation. J Appl Polym Sci 2006; 102: 2107-11. https://doi.org/10.1002/app.24100

[7] Khan A, Aldwayan AS, Alhoshan M, Alsalhi M. Synthesis by *in situ* chemical oxidative polymerization and characterization of polyaniline/iron oxide nanoparticle composite. Polym Int 2010; 59: 1690-4. https://doi.org/10.1002/pi.2908

[8] Umare SS, Shambharkar BH. Synthesis, characterization, and corrosion inhibition study of polyaniline-α-Fe_2O_3 nanocomposite. J Appl Polym Sci 2013; 127: 3349-55. https://doi.org/10.1002/app.37799

[9] Mallikarjuna NN, Manohar SK, Kulkarni PV, Venkataraman A, Aminabhavi TM. Novel high dielectric constant nanocomposites of polyaniline dispersed with γ-Fe_2O_3 nanoparticles. J Appl Polym Sci 2005; 97: 1868-74. https://doi.org/10.1002/app.21405

[10] Bhaumik M, Leswifi TY, Maity A, Srinivasu VV, Onyango MS. Removal of fluoride from aqueous solution by polypyrrole/Fe_3O_4 magnetic nanocomposite. J Hasardous Mater 2011; 186: 150-9. https://doi.org/10.1016/j.jhazmat.2010.10.098

[11] Jokar M, Foroutani R, Safaralizadeh MH, Farhadi K. Synthesis and characterization of polyaniline/Fe_3O_4 magnetic nanocomposite as practical approach for fluoride removal process. Ann Res Rev Biol 2014; 4: 3262-73. https://doi.org/10.9734/ARRB/2014/9108

[12] Shambharkar BH, Umare SS. Production and characterization of polyaniline/Co_3O_4 nanocomposite as a cathode of Zn–polyaniline battery. Mater Sci Eng B 2010; 175: 120-8. https://doi.org/10.1016/j.mseb.2010.07.014

[13] Chen A, Wang H, Zhao B, Wang J, Li X. Preparation and characterization of Fe_3O_4/polypyrrole(PPy) composites. Acta Mater Compos Sin 2004; 21: 157-60.

[14] Aphesteguy JC, Jacobo SE. Composite of polyaniline containing iron oxides. Physica B 2004; 354: 224-7. https://doi.org/10.1016/j.physb.2004.09.053

[15] Wan M, Li J. Synthesis and electrical–magnetic properties of polyaniline composites. J Polym Sci A Polym Chem 1998; 36: 2799-805. https://doi.org/10.1002/(SICI)1099-0518(19981115)36:15<2799::AID-POLA17>3.0.CO;2-1

[16] Zhang Z, Wan M. Nanostructures of polyaniline composites containing nano-magnet. Synth Met 2003; 132: 205-12. https://doi.org/10.1016/S0379-6779(02)00447-2

[17] Karpacheva GP, Ozkan SZh. RU Patent for the invention of "Dispersed nanocomposite magnetic material and method of its obtaining" 2011; № 2426188.

[18] Eremeev IS, Ozkan SZh, Karpacheva GP, Bondarenko GN. Hybrid dispersed magnetic nanomaterial based on polydiphenylamine-2-carbonic acid and Fe_3O_4. Nanotechnologies in Russia 2014; 9: 38-44. https://doi.org/10.1134/S1995078014010054

[19] Karpacheva GP, Ozkan SZh, Eremeev IS, Bondarenko GN, Dzidziguri EL, Chernavskii PA. Synthesis of hybrid magnetic nanomaterial based on polydiphenylamine-2-carboxylic acid and Fe_3O_4 in the interfacial process. Eur Chem Bull 2014; 3: 1001-7.

[20] Karpacheva G, Ozkan S. Polymer-metal hybrid structures based on polydiphenylamine and Co nanoparticles. Procedia Mater Sci 2013; 2: 52-9. https://doi.org/10.1016/j.mspro.2013.02.007

[21] Ozkan SZh, Dzidziguri EL, Chernavskii PA, Karpacheva GP, Efimov MN, Bondarenko GN. Metal-polymer nanocomposites based on polydiphenylamine and cobalt nanoparticles. Nanotechnologies in Russia 2013; 8: 452-60. https://doi.org/10.1134/S1995078013040113

[22] Ozkan SZh, Dzidziguri EL, Karpacheva GP, Chernavskii PA, Efimov MN, Bondarenko GN. A magnetic metal-polymer nanocomposite material based on polydiphenylamine and Fe_3O_4 nanoparticles. Russ Chem Bull 2015; 64: 196-201. https://doi.org/10.1007/s11172-015-0842-5

[23] Karpacheva GP, Ozkan SZh, Dzidziguri EL, *et al.* Hybrid metal-polymer nanocomposites based on polyphenoxazine and cobalt nanoparticles. Eur Chem Bull 2015; 4: 135-41.

[24] Karpacheva GP, Ozkan SZh. RU patent for the invention of "Polymer dispersed magnetic material and method for production thereof", № 2601005 from 27.10.2016

[25] Ozkan SZh, Karpacheva GP, Dzidziguri EL, *et al.* One step synthesis of hybrid magnetic material based on polyphenoxazine and bimetallic Co-Fe nanoparticles. Polym Bull 2016. https://doi.org/10.1007/s00289-016-1878-x

[26] Gubin SP, Koksharov YuA, Khomutov GB, Yurkov GYu. Magnetic nanoparticles: preparation, structure and properties. Rus Chem Rev 2005; 74: 489-520. https://doi.org/10.1070/RC2005v074n06ABEH000897

[27] Chernavskii PA, Pankina GV, Lunin VV. Magnetometric methods of investigation of supported catalysts. Russ Chem Rev 2011; 80: 579-604. https://doi.org/10.1070/RC2011v080n06ABEH004187

[28] Ozkan SZh, Karpacheva GP, Bondarenko GN. Polymers of phenoxazine: synthesis, structure. Russ Chem Bull 2011; 60: 1651-6. https://doi.org/10.1007/s11172-011-0247-z

[29] Massart R. Preparation of aqueous magnetic liquids in alkaline and acidic media. IEEE Trans Magn 1981; 17: 1247-8. https://doi.org/10.1109/TMAG.1981.1061188

[30] Zemtsov LM, Karpacheva GP, Efimov MN, Muratov DG, Bagdasarova KA. Carbon nanostructures based on IR-pyrolyzed polyacrylonitrile. Polym Sci A 2006; 48: 633-7. https://doi.org/10.1134/S0965545X06060125

[31] Dzidziguri EL. Dimensional characteristics of nanopowders. Nanotechnologies in Russia 2009; 4: 857-70. https://doi.org/10.1134/S1995078009110147

[32] Gubin SP. What is nanoparticle? Development trends for nanochemistry and nanotechnology. Ross Khim Zh 2000; 44: 23-31.

Received on 17-10-2016 Accepted on 15-12-2016 Published on 23-01-2017

DOI: http://dx.doi.org/10.6000/1929-5995.2016.05.04.2